Spin-dependent thermoelectric transport through double quantum dots*

Wang Qiang(王 强)[a], Xie Hai-Qing(解海卿)[a], Jiao Hu-Jun(焦虎军)[a], Li Zhi-Jian(李志坚)[a], and Nie Yi-Hang(聂一行)[a)b)†]

[a] *Institute of Theoretical Physics and Department of Physics, Shanxi University, Taiyuan* 030006, *China*
[b] *Institute of Solid State Physics, Shanxi Datong University, Datong* 037009, *China*

(Received 7 April 2012; revised manuscript received 21 May 2012)

We study the thermoelectric transport through a double-quantum-dot system with spin-dependent interdot coupling and ferromagnetic electrodes by means of the non-equilibrium Green's function in the linear response regime. It is found that the thermoelectric coefficients are strongly dependent on the splitting of the interdot coupling, the relative magnetic configurations, and the spin polarization of leads. In particular, the thermoelectric efficiency can reach a considerable value in the parallel configuration when the effective interdot coupling and the tunnel coupling between the quantum dots and the leads for the spin-down electrons are small. Moreover, the thermoelectric efficiency increases with the intradot Coulomb interaction increasing and can reach very high values at appropriate temperatures. In the presence of the magnetic field, the spin accumulation in the leads strongly suppresses the thermoelectric efficiency, and a pure spin thermopower can be obtained.

Keywords: thermoelectric effect, double quantum dots, spin effect

PACS: 73.50.Lw, 65.80.–g, 85.80.Lp, 73.63.Kv **DOI:** 10.1088/1674-1056/21/11/117310

1. Introduction

In recent years, quantum dot (QD) systems as potential artificial thermoelectric devices have attracted much attention, and their thermoelectric properties have been widely studied both experimentally[1−3] and theoretically.[4−36] Due to the deviation from the Wiedemann–Franz law and the suppression of the phonon contributions, the thermoelectric efficiency in the QD system can be significantly enhanced.[4,7] On the other hand, many interesting thermoelectric effects have been observed or predicted in single-QD and double-quantum-dot (DQD) systems in the Coulomb blockade (CB)[4−19] and the Kondo[20−25] regimes. For example, the thermopower and the thermal conductance each as a function of the gate voltage present CB oscillations.[4] The transient thermopower of a single QD system can be strongly enhanced and modified by a time-dependent gate voltage.[10] In a single multilevel QD[11] or a serial-coupled DQD,[13,14] the thermal conductance can be strongly enhanced at a high temperature due to the bipolar effects. When the interference effects are considered in a parallel coupled DQD system, the thermoelectric efficiency can be significantly enhanced by the Fano effect and the Coulomb interaction.[15−18,31] In particular, the strong dependences of thermopower on the temperature and the gate voltage provide a sensitive way to detect and understand the Kondo correlations.[20,22,25]

The recent experimental observation of the spin Seebeck effect[26−28] inspires the research on the spin effects in the energy transport of the QD systems[6−8,29−36] and opens a new way for the thermal manipulation of the spintronic devices and the design of the spin current generator. The spin-dependent thermoelectric effects in single QD and DQD systems connected to two ferromagnetic leads with collinear or noncollinear magnetic configurations have been widely studied in the linear and the nonlinear response regimes.[6−8,14,31−35] The results reveal that the thermoelectric coefficients are strongly dependent on the spin polarization, the relative magnetic configurations of the ferromagnetic leads, and the asymmetry of the dot–lead coupling. Particularly, when the spin-relaxation time of the system is long or an external spin-dependent bias is applied to the sys-

*Project supported by the National Natural Science Foundation of China (Grant Nos. 11274208，10974124, and 11004124) and the Shanxi Natural Science Foundation, China (Grant No. 2009011001-1).

†Corresponding author. E-mail: nieyh@sxu.edu.cn

© 2012 Chinese Physical Society and IOP Publishing Ltd

tem, the spin accumulation in leads can induce a spin-dependent splitting of the chemical potential in the leads.[7,8,31,32,35] As a result, the thermo-spin efficiency can be larger than the thermoelectric efficiency, and a pure spin thermopower can be obtained.[6,31,32] Up to now, most earlier theoretical works about the spin effects in heat transport mainly focus on single QD or parallel coupled DQD systems. More recently, researchers have started to study the thermoelectric effects in a serial-coupled DQD system coupled to ferromagnetic leads.[14] Even so, still much more work is needed to understand the interplay between the spin effect and the heat transport in the serial-coupled DQD system, particularly in the presence of the magnetic field and the spin accumulation in the leads.

In this work, we consider a lateral DQD system with spin-dependent interdot coupling connected to two ferromagnetic electrodes. The spin-dependent interdot coupling can be achieved by applying a static magnetic field on the tunnelling junction between the two QDs, which induces the spin-dependent level splitting. The tunable parameters further enrich the thermoelectronic and the thermo-spin transport properties in the DQD system. By using the nonequilibrium Green's function technique, the thermoelectric and the thermo-spin coefficients are obtained. It is found that in the parallel configuration, the thermoelectric efficiency can reach a considerable value around the spin-down resonance levels when the effective interdot coupling and the tunnel coupling between the QDs and the leads for the spin-down electrons are small. On the other hand, in the presence of the magnetic field, the spin accumulation in the leads strongly suppresses the thermoelectric efficiency. In particular, the thermoelectric and the thermo-spin efficiencies are strongly enhanced by the intradot Coulomb interactions and can reach very high values at appropriate temperatures. Moreover, a pure spin thermopower can be obtained.

The rest of this work is organized as follows. In Section 2, we introduce the model for the lateral DQD system with spin-dependent interdot coupling and derive the basic analytical formulas. In Section 3, we present the corresponding numerical results about the influences of the related parameters on the thermoelectric and the thermospin properties of the present device. Finally, in Section 4, we summarize the work.

2. Model and formalism

We consider a lateral DQD system with spin-dependent interdot coupling and two ferromagnetic leads. The magnetizations of the leads are assumed to be collinear, and can be either in the parallel or antiparallel configuration. The Hamiltonian describing the system can be decomposed into three parts, i.e., $H = H_{\rm d} + H_{\alpha} + H_{\rm T}$. The first term describes the isolated DQD and is given by

$$H_{\rm d} = \sum_{m\sigma} \varepsilon_{m\sigma} d^{\dagger}_{m\sigma} d_{m\sigma} + \sum_{m} U n_{m\sigma} n_{m\bar{\sigma}} - \sum_{\sigma} \left[(t + \delta_{\sigma} \Delta t) \left(d^{\dagger}_{1\sigma} d_{2\sigma} + d^{\dagger}_{2\sigma} d_{1\sigma} \right) \right], \quad (1)$$

where operator $d^{\dagger}_{m\sigma}$ ($d_{m\sigma}$) creates (annihilates) an electron with energy $\varepsilon_{m\sigma}$ and spin σ in QD m, U is the intradot Coulomb interaction constant, and $n_{m\sigma} = d^{\dagger}_{m\sigma} d_{m\sigma}$ is the particle number operator. We assume that the level spacing is very large, so we only need to consider one single energy level in each QD. The last term in Eq. (1) describes the spin-dependent tunnelling between the two QDs, where δ_{σ} is defined as $\delta_{\sigma} = 1$ for $\sigma = \uparrow$ and $\delta_{\sigma} = -1$ for $\sigma = \downarrow$. The spin-dependent tunnelling can be induced by a static magnetic field applied to the barrier region between the two QDs. When electrons pass through the potential barrier region, the electron with spin parallel to the magnetic field has a larger tunnelling probability than the one with spin antiparallel to the magnetic field due to the Larmor precession of the electron spin inside the potential barrier.[37−40]

The second term H_{α} describes the noninteracting electrons in the leads and is written as $H_{\alpha} = \sum_{\alpha={\rm L,R}} \sum_{k\sigma} \varepsilon_{k\alpha} c^{\dagger}_{k\alpha\sigma} c_{k\alpha\sigma}$, where $c^{\dagger}_{k\alpha\sigma}$ ($c_{k\alpha\sigma}$) creates (annihilates) a conduction electron with energy $\varepsilon_{k\alpha}$, momentum k, and spin σ in the α electrode. The third term of the Hamiltonian describes the coupling between the DQD and the electrodes, and reads $H_{\rm T} = \sum_{k\sigma} (V_{\rm L1\sigma} c^{\dagger}_{kL\sigma} d_{1\sigma} + V_{\rm R2\sigma} c^{\dagger}_{kR\sigma} d_{2\sigma} + {\rm H.c})$, where $V_{\alpha m\sigma}$ is the hopping matrix element between QD m and electrode α, which is assumed to be independent of momentum k. In the following calculation, we define the line-width matrix as $\Gamma^{\sigma}_{nm\alpha} = V_{\alpha n\sigma} V^{*}_{\alpha m\sigma} \sum_{k} 2\pi\delta(\omega - \varepsilon_{k\alpha})$, $(\alpha = {\rm L, R})$. In the wide-band limit, $\Gamma^{\alpha}_{nm\sigma}$ is independent of the energy. Using the matrix representation, we have

$$\boldsymbol{\Gamma}^{\sigma}_{\rm L} = \begin{pmatrix} \Gamma^{\sigma}_{11L} & \Gamma^{\sigma}_{12L} \\ \Gamma^{\sigma}_{21L} & \Gamma^{\sigma}_{22L} \end{pmatrix} = \begin{pmatrix} \Gamma^{\sigma}_{\rm 1L} & 0 \\ 0 & 0 \end{pmatrix},$$

$$\boldsymbol{\Gamma}_{\mathrm{R}}^{\sigma}=\begin{pmatrix}\Gamma_{11R}^{\sigma} & \Gamma_{12R}^{\sigma}\\ \Gamma_{21R}^{\sigma} & \Gamma_{22R}^{\sigma}\end{pmatrix}=\begin{pmatrix}0 & 0\\ 0 & \Gamma_{2\mathrm{R}}^{\sigma}\end{pmatrix}, \tag{2}$$

with $\Gamma_{1\mathrm{L}}^{\sigma}=\Gamma_{11L}^{\sigma}$ and $\Gamma_{2\mathrm{R}}^{\sigma}=\Gamma_{22R}^{\sigma}$. When the spin polarization of the leads is considered, the matrix element may be assumed to be in the form $\Gamma_{1\mathrm{L}}^{\sigma}=\Gamma_{\mathrm{L}}(1+\delta_{\sigma}p_{\mathrm{L}})$ and $\Gamma_{2\mathrm{R}}^{\sigma}=\Gamma_{\mathrm{R}}(1\pm\delta_{\sigma}p_{\mathrm{R}})$ with + (−) for the parallel (antiparallel) alignment of the magnetization in the two electrodes. The p_{α} is related to the lead's spin polarization, while Γ_{α} describes the tunnelling coupling between the DQD and the α electrode when $p_{\alpha}=0$. In the following calculation, we assume $p_{\mathrm{L}}=p_{\mathrm{R}}=p$ and $\Gamma_{\mathrm{L}}=\Gamma_{\mathrm{R}}=\Gamma$.

By using the nonequilibrium Green's function technique, the electric and heat currents from the α lead flowing into the QDs can be written as[13,41]

$$\begin{aligned}I_{\alpha}&=\sum_{\sigma}I_{\alpha\sigma}\\&=\sum_{\sigma}\frac{e}{\hbar}\int\frac{\mathrm{d}\omega}{2\pi}\left[f_{\alpha}(\omega)-f_{\beta}(\omega)\right]T_{\sigma}(\omega),\end{aligned} \tag{3}$$

$$\begin{aligned}I_{Q\alpha}=&\sum_{\sigma}\frac{1}{\hbar}\int\frac{\mathrm{d}\omega}{2\pi}(\omega-\mu_{\alpha})\left[f_{\alpha}(\omega)\right.\\&\left.-f_{\beta}(\omega)\right]T_{\sigma}(\omega),\end{aligned} \tag{4}$$

where $\beta\neq\alpha$, and $f_{\alpha}=[\mathrm{e}^{(\omega-\mu_{\alpha})/k_{\mathrm{B}}T_{\alpha}}+1]^{-1}$ is the Fermi distribution function for the α electrode with chemical potential μ_{α}, temperature T_{α}, and Boltzmann constant k_{B}. The $T_{\sigma}(\omega)$ is the transmission coefficient corresponding to spin channel σ and is given by

$$T_{\sigma}(\omega)=\mathrm{Tr}\left[G_{\sigma}^{\mathrm{a}}(\omega)\Gamma_{\mathrm{R}}^{\sigma}G_{\sigma}^{\mathrm{r}}(\omega)\Gamma_{\mathrm{L}}^{\sigma}\right], \tag{5}$$

where $G_{\sigma}^{\mathrm{r}}(\omega)$ and $G_{\sigma}^{\mathrm{a}}(\omega)$ are the retarded and advanced Green's functions in the DQD, respectively, with $G_{\sigma}^{\mathrm{a}}(\omega)=[G_{\sigma}^{\mathrm{r}}(\omega)]^{\dagger}$. By employing the equation of motion and adopting the Hartree–Fock truncation approximation for higher order Green's functions, the retarded Green's function can be obtained from the Dyson equation as[42]

$$\begin{aligned}G_{\sigma}^{\mathrm{r}}(\omega)&=\begin{pmatrix}G_{11\sigma}^{\mathrm{r}}(\omega) & G_{12\sigma}^{\mathrm{r}}(\omega)\\ G_{21\sigma}^{\mathrm{r}}(\omega) & G_{22\sigma}^{\mathrm{r}}(\omega)\end{pmatrix}\\&=g_{\sigma}^{\mathrm{r}}(\omega)+g_{\sigma}^{\mathrm{r}}(\omega)\Sigma_{\sigma}^{\mathrm{r}}G_{\sigma}^{\mathrm{r}}(\omega),\end{aligned} \tag{6}$$

where $\Sigma_{\sigma}^{\mathrm{r}}=-\mathrm{i}\left[\Gamma_{\mathrm{R}}^{\sigma}+\Gamma_{\mathrm{L}}^{\sigma}\right]$ is the retarded self-energy in the wide-band limit, and $g_{\sigma}^{\mathrm{r}}(\omega)$ is the retarded Green's function for the isolated DQD (without coupling to the electrodes), which is expressed as

$$g_{\sigma}^{\mathrm{r}}(\omega)=\begin{bmatrix}C_{1\sigma} & t+\delta_{\sigma}\Delta t\\ t+\delta_{\sigma}\Delta t & C_{2\sigma}\end{bmatrix}^{-1}, \tag{7}$$

with $C_{m\sigma}=(\omega-\varepsilon_{m\sigma}-U)(\omega-\varepsilon_{m\sigma})/(\omega-\varepsilon_{m\sigma}-U+Un_{m\bar{\sigma}})$. The $n_{m\bar{\sigma}}$ is the averaged occupation number of electrons with spin $\bar{\sigma}$ in the m quantum dot, and can be calculated self-consistently by using the formula

$$n_{m\bar{\sigma}}=\left\langle d_{m\bar{\sigma}}^{\dagger}d_{m\bar{\sigma}}\right\rangle=-\mathrm{i}\int\frac{\mathrm{d}\omega}{2\pi}G_{m\bar{\sigma},m\bar{\sigma}}^{<}(\omega),$$

where $G_{\sigma}^{<}(\omega)$ is the lesser Green's function and can be obtained by using the Keldysh equation $G_{\sigma}^{<}(\omega)=G_{\sigma}^{\mathrm{r}}(\omega)\Sigma_{\sigma}^{<}(\omega)G_{\sigma}^{\mathrm{a}}(\omega)$ with the lesser self-energy $\Sigma_{\sigma}^{<}(\omega)=\mathrm{i}[f_{\mathrm{L}}(\omega)\Gamma_{\mathrm{L}}^{\sigma}+f_{\mathrm{R}}(\omega)\Gamma_{\mathrm{R}}^{\sigma}]$. It should be pointed out that the Hartree–Fock decoupling approximation scheme is reasonable when the temperature in our calculation is higher than the Kondo temperature.

In the linear response regime, the spin accumulation in the electrodes can be neglected when the spin relaxation time is sufficiently short.[7,31,32,35] In this case, the voltage induced by a temperature gradient can be treated as independent of spin. The electric and the heat currents through the system can be written as

$$I=e^{2}L_{0}\Delta V+\frac{eL_{1}}{T}\Delta T, \tag{8}$$

$$I_{Q}=-eL_{1}\Delta V-\frac{L_{2}}{T}\Delta T, \tag{9}$$

with

$$L_{n}=-\sum_{\sigma}\frac{1}{\hbar}\int\frac{\mathrm{d}\omega}{2\pi}(\omega-\mu)^{n}\frac{\partial f(\omega,\mu,T)}{\partial\omega}T_{\sigma}(\omega).$$

In the following calculation, we assume $\mu_{\mathrm{L}}=\mu_{\mathrm{R}}$ and $T_{\mathrm{L}}=T_{\mathrm{R}}$, thus the Fermi distribution function is $f_{\alpha}(\omega)=f(\omega)$. The electric and the thermal conductances can be calculated by formulas $G=e^{2}L_{0}$ and $\kappa=\frac{1}{T}[L_{2}-\frac{L_{1}^{2}}{L_{0}}]$, respectively. The thermopower is defined as the thermoelectric voltage ΔV induced by a temperature gradient ΔT under the condition of $I=0$, i.e., $S=\frac{\Delta V}{\Delta T}=-\frac{1}{eT}\frac{L_{1}}{L_{0}}$. The thermoelectric conversation efficiency of the system is described by the dimensionless figure of merit (FOM) $ZT=GS^{2}T/(\kappa_{\mathrm{ph}}+\kappa)$, where κ_{ph} denotes the phonon contribution to the thermal conductance, which is suppressed in our DQD–electrodes structure, and is ignored in this paper.

If the spin relaxation time of the system is sufficiently long, the spin accumulation in the electrodes should be considered,[7,31,32,35] which leads to the chemical potential difference ΔV_{σ} between the two leads which is related to the spin channel. Thus, in this system, we can define a spin bias ΔV_{s} induced by

the temperature gradient, i.e., $\Delta V_\sigma = \Delta V + \delta_\sigma \Delta V_{\rm s}$. Corresponding spin-resolved electric and heat currents can be expressed as

$$I_\sigma = e^2 L_0^\sigma \Delta V_\sigma + e\frac{L_1^\sigma}{T}\Delta T, \tag{10}$$

$$I_Q = -\sum_\sigma \left(eL_1^\sigma \Delta V_\sigma + \frac{L_2^\sigma}{T}\Delta T \right), \tag{11}$$

where

$$L_n^\sigma = -\frac{1}{\hbar}\int \frac{{\rm d}\omega}{2\pi}(\omega-\mu)^n \frac{\partial f_\sigma(\omega,\mu,T)}{\partial \omega} T_\sigma(\omega), \quad (n=0,1,2).$$

The charge and the spin conductances can be calculated as $G = e^2[L_0^\uparrow + L_0^\downarrow]$ and $G_{\rm s} = e^2[L_0^\uparrow - L_0^\downarrow]$, respectively, while the thermal conductance is given by $\kappa = -\sum_\sigma \frac{1}{T}[L_2^\sigma - \frac{L_1^\sigma L_1^\sigma}{L_0^\sigma}]$, which is identical to the value without spin accumulation in such a system. We may introduce from Eq. (10) the spin-dependent thermopower $S_\sigma = \frac{\Delta V_\sigma}{\Delta T} = -\frac{1}{eT}\frac{L_1^\sigma}{L_0^\sigma}$ in spin channel σ under the condition of current I_σ vanishing. Then the charge and the spin thermopowers are defined as $S_{\rm c} = \frac{\Delta V}{\Delta T} = \frac{1}{2}[S_\uparrow + S_\downarrow]$ and $S_{\rm s} = \frac{\Delta V_{\rm s}}{\Delta T} = \frac{1}{2}[S_\uparrow - S_\downarrow]$, respectively. The corresponding charge and spin figures of merit are defined as $ZT_{\rm c} = \frac{GS_{\rm c}^2 T}{\kappa}$ and $ZT_{\rm s} = \left|\frac{G_{\rm s}S_{\rm s}^2 T}{\kappa}\right|$, respectively, which describe the heat-to-charge-voltage and the heat-to-spin-voltage conversion efficiencies of the present system when the spin accumulation is considered. The $ZT_{\rm s}$ has the form of absolute value because the spin conductance may be negative in some regions.

3. Numerical results and discussion

In the following, we show the numerical results of the spin-dependent thermoelectric effects in the DQD system based on the above formulas. Three cases are studied: without spin accumulation in the leads and $U = 0$, without spin accumulation in the leads and $U \neq 0$; and with spin accumulation in the leads. For simplicity, we assume that the two QDs have the same bare energy levels $\varepsilon_{m\sigma}$ and $\varepsilon_{m\sigma} = \varepsilon$, which can be realized by tuning the gate voltage in the experiment. The relevant parameters are chosen as $\mu_{\rm L} = \mu_{\rm R} = 0$, $T_{\rm L} = T_{\rm R} = T$, $\Gamma = 0.1$ meV, and $t = 2$ meV.

3.1. Without spin accumulation and $U = 0$

Consider the case that the magnetizations of the leads are in the parallel configuration, there is no spin accumulation in the leads, and the intradot Coulomb interactions are ignored. The tunnel coupling between the two QDs is spin-dependent due to the external magnetic field, such a coupling DQD can be equivalent to a single QD with four spin-dependent levels, $E_{1\uparrow} = \varepsilon + t + \Delta t$, $E_{2\uparrow} = \varepsilon - t - \Delta t$, $E_{3\downarrow} = \varepsilon + t - \Delta t$, and $E_{4\downarrow} = \varepsilon - t + \Delta t$, which correspond to the poles of the Green function $g_\sigma^{\rm r}(\omega)$ given by Eq. (7). These levels are identified as $E_{u\uparrow}$ $(u = 1, 2)$ occupied by the spin-up electrons and $E_{d\downarrow}$ $(d = 3, 4)$ occupied by the spin-down electrons, and satisfy $E_{1\uparrow} > E_{3\downarrow} > E_{4\downarrow} > E_{2\uparrow}$ for the chosen parameters.

The influence of splitting Δt of the interdot coupling on the thermoelectric transport is shown in Fig. 1. Four resonance peaks appear in the electrical conductance spectrum when the spin-dependent level crosses the Fermi level ($\mu = 0$), see Fig. 1(a). It can be clearly seen that the change of Δt only changes the electrical conductance's resonance position and does not influence its magnitude. This is also true for the thermal conductance κ at low temperatures. However, the behaviour of κ is more complicated at relatively high temperatures (shown in Fig. 1(b)). While the thermopower S and the figure of merit ZT are more sensitive to the change of Δt. The antisymmetry, oscillation, and sign reversal of S are found in Fig. 1(c). As shown in Fig. 1(d), ZT presents the typical double-peak structure. When Δt increases, for the two ZT peaks around $\epsilon = E_{d\downarrow}$, not only do their magnitudes augment, but also their degree of asymmetry increases. In particular, ZT exhibits a behaviour similar to a crossover and can reach a very high value when Δt is close to t (see the inset of Fig. 1(d)). This is because when Δt is close to t, levels $E_{3\downarrow}$ and $E_{4\downarrow}$ get much closer to each other, and the spin-down resonance channels are significantly blockaded due to the strong reduction of the interdot tunnelling for the spin-down electrons. While with the increasing Δt, the side peaks located at $\epsilon = E_{d\uparrow}$ only shift their positions without changing their maxima.

Next, we study the influence of spin polarization p on the thermoelectric transport. The relevant thermoelectric coefficients versus the dot's level ε for different spin polarization p are presented in Fig. 2. When p increases, the electrical and the thermal conductance peaks (the thermopower peaks) located at $\epsilon = E_{u\uparrow}$ increase (decrease) while those (the thermopower ones) located at $\epsilon = E_{d\downarrow}$ decrease (increase), because $\Gamma_{\rm 1L}^\uparrow$, $\Gamma_{\rm 2R}^\uparrow$ increase and $\Gamma_{\rm 1L}^\downarrow$, $\Gamma_{\rm 2R}^\downarrow$ decrease. These properties of G, κ, and S determine the behaviour of ZT. As

shown in Fig. 2(d), with increasing p, the ZT near $\epsilon = E_{u\uparrow}$ is suppressed, while that near $\epsilon = E_{d\downarrow}$ is intensively enhanced. The dependence of ZT on the spin polarization in the leads and the spin-dependent levels may be useful for designing spin-dependent thermoelectric devices. However, it should be noted that when the spin polarization in the leads is very high, for example, $p > 0.95$, the tunnelling rate for the spin-down electrons is close to zero, leading to a significant suppression of the transport through the spin-down levels. Thus, the corresponding ZT peaks rapidly decrease with the increase of p, which can be clearly seen from the inset (ii) of Fig. 2(d).

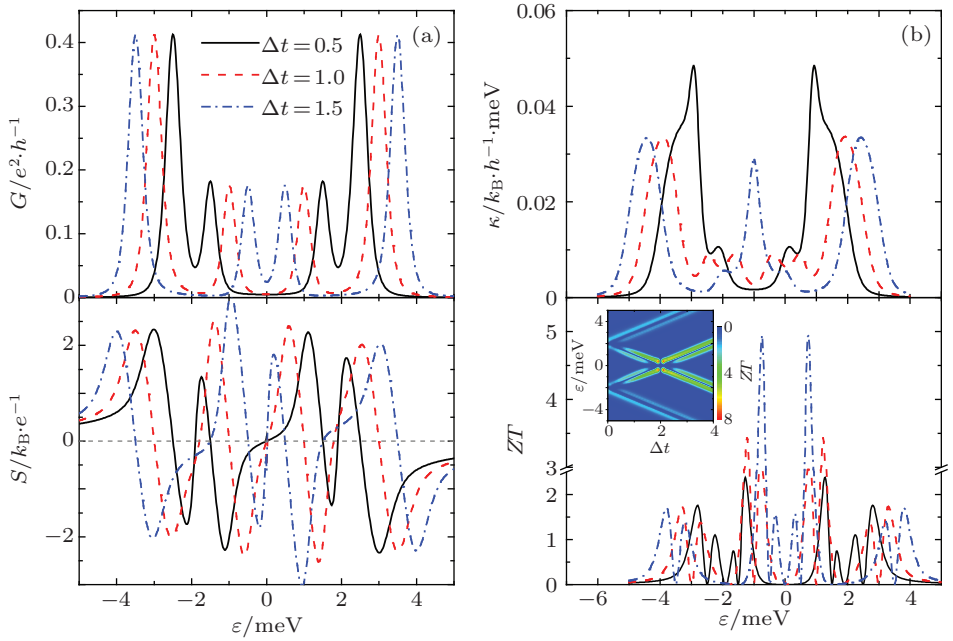


Fig. 1. (colour online) Thermoelectric coefficients (a) G, (b) κ, (c) S, and (d) ZT versus the dot's level ε for various splitting Δt in the parallel configuration with $k_{\rm B}T = 0.1$ meV. The Δt is in units of meV. The other parameters are $t = 2$ meV, $U = 0$ meV, $\Gamma = 0.1$ meV, and $p = 0.5$. The inset in panel (d) depicts ZT as a function of ε and Δt.

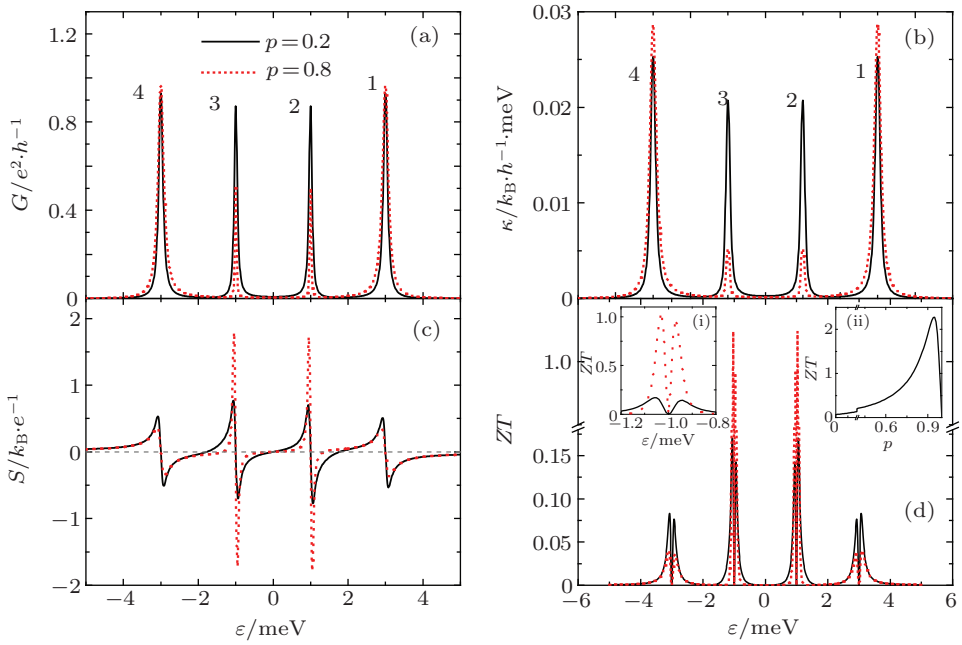


Fig. 2. (colour online) Thermoelectric coefficients (a) G, (b) κ, (c) S, and (d) ZT versus dot's level ε for different spin polarization p in the parallel configuration with $k_{\rm B}T = 0.01$ meV and $\Delta t = 1$ meV. The other parameters are the same as those in Fig. 1. Inset (i) is an enlargement of the region near $\varepsilon = -1$ meV. Inset (ii) depicts ZT as a function of spin polarization p at $\varepsilon = -1.03$ meV.

When the magnetic configuration changes from parallel to antiparallel, the electrical conductances are suppressed in the four resonance channels, but the changes of thermal conductance κ and thermopower S are dependent on the resonance levels (see Fig. 3). The κ (S) lowers (heightens) in the spin-up resonance channels and heightens (lowers) in the spin-down resonance channels. As a result, ZT in the antiparallel configuration presents higher peaks around the spin-up resonance channels and lower peaks around spin-down resonance channels compared with those in the parallel configuration. In the antiparallel configuration, the tunnelling rates between the leads and the QDs satisfy $\Gamma_{1\mathrm{L}}^{\uparrow}\Gamma_{2\mathrm{R}}^{\uparrow} = \Gamma_{1\mathrm{L}}^{\downarrow}\Gamma_{2\mathrm{R}}^{\downarrow}$, which leads to the transmission coefficient $T_\sigma(\omega) = |G_{\sigma 12}^{\mathrm{r}}(\omega)|^2\Gamma_{1\mathrm{L}}^{\sigma}\Gamma_{2\mathrm{R}}^{\sigma}$ being spin-independent. Then the thermoelectric quantities have the same intensities at different resonance points. Although the electric and the thermal conductances experience a decreasing trend with the increasing p, the thermopower and the figure of merit are independent of p. Based on the above discussion, in order to obtain a high thermoelectric efficiency, we can tune the resonance points to spin-down levels and take $p \sim 0.9$ in the parallel configuration for fixed temperature and splitting of the interdot coupling.

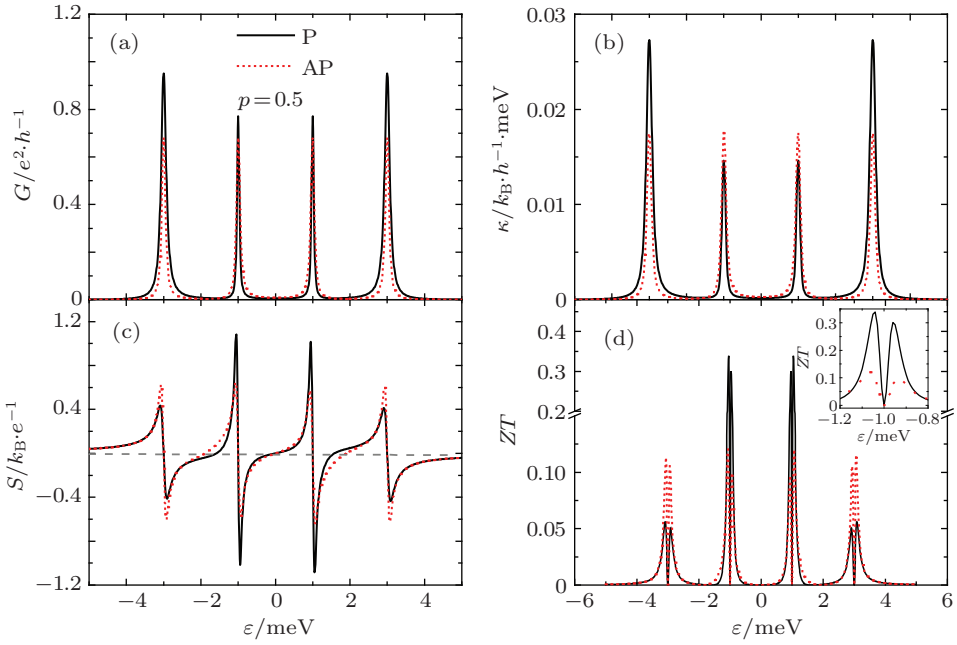


Fig. 3. (colour online) Thermoelectric coefficients (a) G, (b) κ, (c) S, and (d) ZT versus dot's level ε in the antiparallel and the parallel configurations with $p = 0.5$. The other parameters are the same as those in Fig. 2. Inset is the enlargement of the region near $\varepsilon = -1$ meV.

3.2. Without spin accumulation and $U \neq 0$

Now we focus on the case taking into account the intradot Coulomb interactions. Under the Hartree–Fock approximation, such a coupling DQD system is equivalent to a single QD with eight energy levels, in which four levels are occupied by the spin-up electrons and the other four are occupied by the spin-down electrons.[37] To determine the eight spin-dependent effective energy levels, we need to solve self-consistently the equation $\left|[g_\sigma^{\mathrm{r}}(\omega)]^{-1}\right| = 0$ due to $U \neq 0$. Figure 4 presents the relevant thermoelectric quantities versus the dot's level ε with different temperatures and $U = 5$ meV. At low temperatures, eight resonance peaks of G and κ can be clearly seen in Figs. 4(a) and 4(b). The peaks 1, 4, 5, 8 (2, 3, 6, 7) correspond to the electron transport through the spin-up (down) resonance channels. With the temperature increasing, the conductance peaks become wider and lower due to the broadening of the Fermi distribution function. More interestingly, at high temperatures, the thermal conductance presents five high peaks due to the bipolar effects.[11,13]

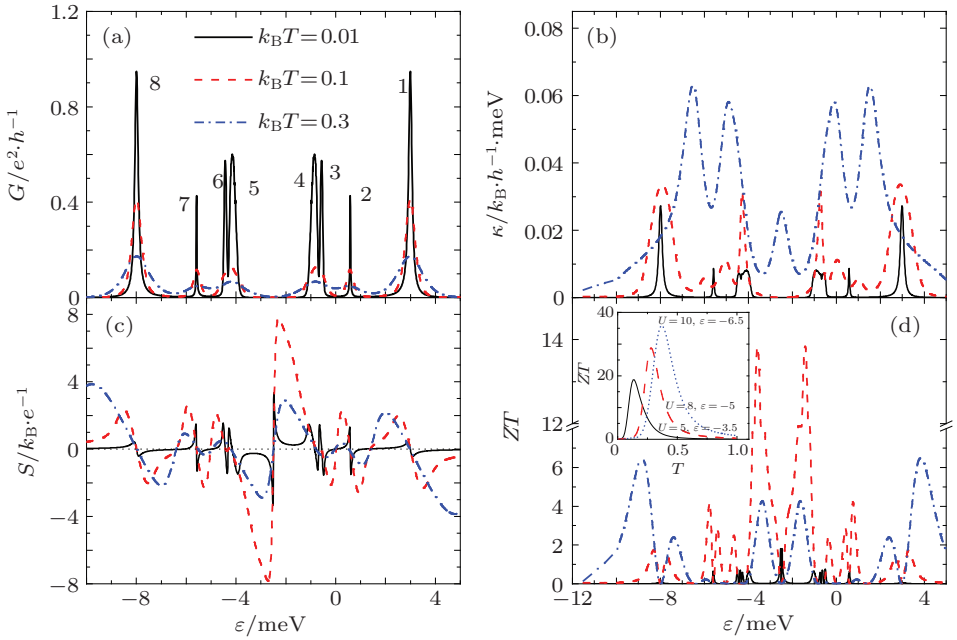


Fig. 4. (colour online) Thermoelectric coefficients (a) G, (b) κ, (c) S, and (d) ZT versus dot's level ε for various temperature T in the parallel configuration with $U = 5$ meV and $p = 0.5$. The k_BT is in units of meV. The other parameters are the same as those in Fig. 2.

The S and ZT experience nonmonotonous variation trends with the increasing temperature (see Figs. 1(c) and 1(d)). In particular, at high temperatures, two high peaks of ZT appear near the symmetry point $\varepsilon = -U/2$, resulting from a suppression of κ and an enhancement of S. Comparing with the case in the absence of U, it can be found that the Coulomb interactions shift the positions of the peaks of ZT and strongly enhance ZT. As shown in the insert of Fig. 4(d), the maximum of ZT increases with the increasing Coulomb interactions and can reach very high values above 30 at appropriate temperatures, which is very useful for thermoelectric energy conversion devices. It should be mentioned that for varying the relative magnetic configurations and spin polarization of leads, the relevant thermoelectric quantities exhibit the same variation trend as that without the Coulomb interactions, except for the peaks around $\varepsilon = -U/2$, which are unaffected.

3.3. With spin accumulation

For the systems with a long spin relaxation time, the spin accumulation in the electrodes should be considered.[7,31,35] Figure 5 presents the thermoelectric coefficients versus ε in the presence of spin accumulation. It is found by comparing Fig. 3 with Fig. 5 that the spin accumulation in the electrodes has no influence on the electrical and the thermal conductances (not shown) but strongly influences the thermopower and the figure of merit. The peaks of S_c and ZT_c are much lower than the corresponding ones in S and ZT. These properties are quite different from those in the absence of an external magnetic field, i.e., the splitting of interdot coupling $\Delta t = 0$. Since the levels are strongly spin-dependent in the system, the spin FOM experiences the same variation trend as the charge FOM with the varying relative magnetic configurations and spin polarization of the leads, and the behaviours are similar to those in the case without spin accumulation discussed above.

Some novel properties also appear, for instance, in the absence of the Coulomb interactions, $G_s = -G$ at resonance point $\epsilon = E_{d\downarrow}$, while $G_s = G$ at resonance point $\epsilon = E_{d\uparrow}$ (see Fig. 5(a)). More interestingly, for certain ε (pointed by the arrows around $\varepsilon = \pm t$ in Fig. 5(b)), the charge thermopower vanishes, while the spin thermopower can be finite, because the thermopowers for different spins have the same value but opposite signs, which means that a pure spin current without charge current may be produced by a temperature gradient in our system. This feature can also be obtained in the spectrum of figure of merit shown in Fig. 5(c). When the Coulomb interaction is considered, near the symmetry point, ZT_c exhibits two very high peaks, while ZT_s completely vanishes. This is because the thermopowers for different spins have the same value and sign, leading to the enhancement

of the charge thermopower and the suppression of the spin thermopower. Even so, ZT_c and ZT_s are strongly enhanced by the Coulomb interactions, and ZT_s can be larger than ZT_c for selected dot level positions in the Coulomb blockade regime. This implies that our system is a good heat-to-spin-voltage converter.

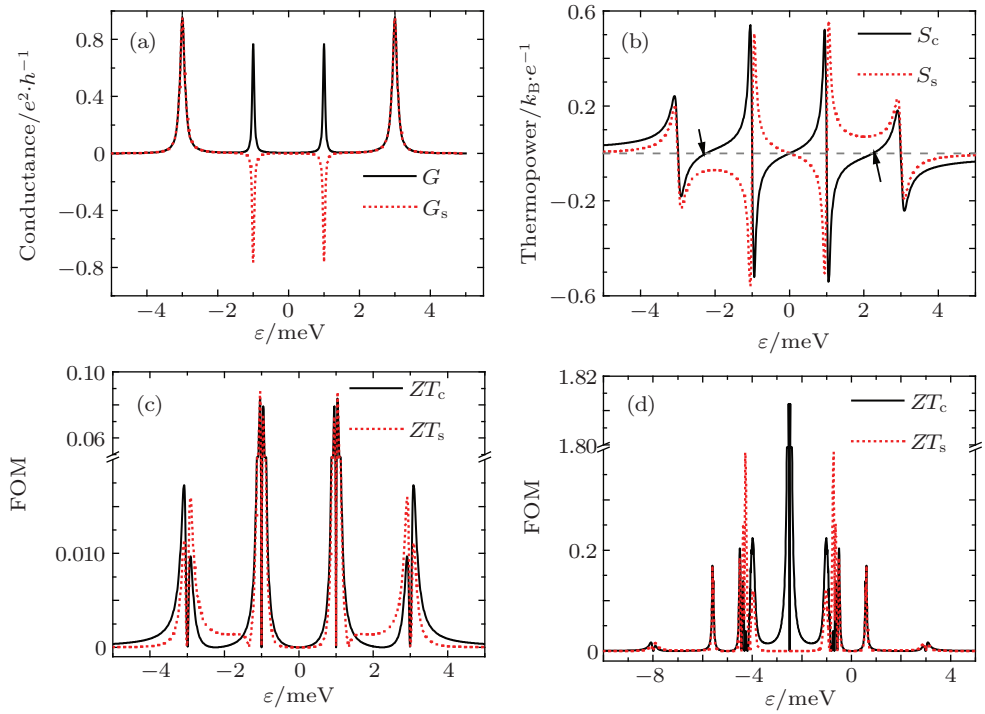


Fig. 5. (colour online) (a) Electrical conductance G and spin conductance G_s, (b) thermopower S and spin thermopower S_s, and ((c) (d)) charge figure of merit ZT_c and spin figure of merit ZT_s versus ε in the parallel configuration with $p = 0.5$. The Coulomb interactions are $U = 0$ meV in panels (a), (b), (c) and $U = 5$ meV in panel (d). The other parameters are the same as those in Fig. 2.

4. Conclusion

In summary, we study the spin effects in thermoelectric transport through a lateral DQD system with spin dependent interdot coupling and ferromagnetic electrodes. It is found that in the parallel configuration, the thermoelectric efficiency can reach a considerable value around the spin-down resonance levels when the effective interdot coupling and the tunnel coupling between the QDs and the leads for the spin-down electrons are small. On the other hand, in the presence of the magnetic field, the spin accumulation in the leads strongly suppresses the thermoelectric efficiency. The thermoelectric and the thermospin efficiencies are strongly enhanced by the intradot Coulomb interactions and can reach very high values at appropriate temperatures. Moreover, a pure spin thermopower can be obtained in such a DQD system.

References

[1] Harman T C, Taylor P J, Walsh M P and LaForge B E 2002 *Science* **297** 2229
[2] Scheibner R, Buhmann H, Reuter D, Kiselev M N and Molenkamp L W 2005 *Phys. Rev. Lett.* **95** 176602
[3] Scheibner R, Konig M, Reuter D, Wieck A D, Buhmann H and Molenkamp L W 2008 *New J. Phys.* **10** 083016
[4] Zianni X 2007 *Phys. Rev.* B **75** 045344
[5] Chen X O, Dong B and Lei X L 2008 *Chin. Phys. Lett.* **25** 3032
[6] Dubi Y and Ventra M Di 2009 *Phys. Rev.* B **79** 081302(R)
[7] Świrkowicz R, Weirzbicki M and Barna's J 2009 *Phys. Rev.* B **80** 195409
[8] Świrkowicz R, Weirzbicki M and Barna's J 2010 *J. Phys. Conf. Ser.* **213** 012021
[9] Weirzbicki M and Świrkowicz R 2010 *J. Phys.: Condens. Matter* **22** 185302
[10] Crepieux A, Simkovic F, Cambon B and Michelini F 2011 *Phys. Rev.* B **83** 153417
[11] Liu J, Sun Q F and Xie X C 2010 *Phys. Rev.* B **81** 245323
[12] Kuo D M T and Chang Y C 2010 *Phys. Rev.* B **81** 205321
[13] Chi F, Zheng J, Lu X D and Zhang K C 2011 *Phys. Lett.* A **375** 1352
[14] Tagani M B and Soleimani H R 2012 *Physica B* **152** 914

[15] Rajput G, Ahluwalia P K and Sharma K C 2011 *Physica* B **406** 3328
[16] Liu Y S and Yang X F 2010 *J. Appl. Phys.* **108** 023701
[17] Liu Y S, Zhang D B, Yang X F and Feng J F 2011 *Nanotechnology* **22** 225201
[18] Weirzbicki M and Świrkowicz R 2011 *Phys. Rev.* B **84** 075410
[19] Xue H J, Lü T Q, Zhang H C, Yin H T, Cui L and He Z L 2011 *Chin. Phys.* B **20** 027301
[20] Boese D and Fazio R 2001 *Europhys. Lett.* **56** 576
[21] Kim T S and Hershfield S 2002 *Phys. Rev. Lett.* **88** 136601
[22] Krawiec M and Wysokinski K I 2007 *Phys. Rev.* B **75** 155330
[23] Zhang Z Y 2007 *J. Phys.*: *Condens. Matter* **19** 086214
[24] Franco R, Valencia J S and Figueira M S 2008 *J. Appl. Phys.* **103** 07B726
[25] Schops V, Zlatić V and Costi T A 2010 *Phys. Rev.* B **81** 235127
[26] Uchida K, Takahashi S, Harii K, Ieda J, Koshibae W, Ando K, Maekawa S and Saitoh E 2008 *Nature* **455** 778
[27] Slachter A, Bakker F L, Adam J P and vanWees B J 2010 *Nat. Phys.* **6** 879
[28] Jaworski C M, Yang J, Mack S, Awschalom D D, Heremans J P and Myers R C 2010 *Nat. Mater.* **9** 898
[29] Wang R Q, Sheng L, Shen R, Wang B G and Xing D Y 2010 *Phys. Rev. Lett.* **105** 057202
[30] Qi F H, Ying Y B and Jin G J 2011 *Phys. Rev.* B **83** 075310
[31] Weirzbicki M and Świrkowicz R 2010 *Phys. Rev.* B **82** 165334
[32] Weirzbicki M and Świrkowicz R 2011 *Phys. Lett.* A **375** 609
[33] Zhu L C, Jiang X D, Zu X T and Lü H F 2010 *Phys. Lett.* A **374** 4269
[34] Liu Y S, Yang X F and Feng J F 2011 *J. Appl. Phys.* **109** 053712
[35] Trocha P and Barna's J 2012 *Phys. Rev.* B **85** 085408
[36] Xue H J, Lü T Q, Zhang H C, Yin H T, Cui L and He Z L 2012 *Chin. Phys.* B **21** 037201
[37] Li Z J, Jin Y H, Nie Y H and Liang J Q 2008 *J. Phys.*: *Condens. Matter* **20** 085214
[38] Wang H X, Y W and Wang F W 2011 *J. Appl. Phys.* **109** 053710
[39] Buttiker M 1983 *Phys. Rev.* B **27** 6178
[40] Huttel A K, Ludwig S, Lorenz H, Eberl K and Kotthaus J P 2005 *Phys. Rev.* B **72** 081310
[41] Haug H and Jauho A P 2008 *Quantum Kinetics in Transport and Optics of Semiconductors* (2nd edn.)(Berlin: Springer-Verlag) pp. 181–210
[42] Yin H T, Lü T Q, Liu X J and Xue H J 2009 *Chin. Phys. Lett.* **26** 047302